

# Tuning the Order of the Nonequilibrium Quantum Phase Transition in a Hybrid Atom-Optomechanical System

Niklas Mann<sup>1</sup>, Axel Pelster<sup>2</sup>, and Michael Thorwart<sup>1</sup>

<sup>1</sup>*I. Institut für Theoretische Physik, Universität Hamburg, Jungiusstraße 9, 20355 Hamburg, Germany*

<sup>2</sup>*Physics Department and Research Center OPTIMAS, Technische Universität Kaiserslautern, Erwin-Schrödinger Straße 46, 67663 Kaiserslautern, Germany*

(Dated: 02:49, Sunday 15<sup>th</sup> December, 2024)

A quantum many-body hybrid system is considered formed by a nanomembrane in an optical cavity, the outcoupled light of which provides a lattice for an ultracold atomic Bose gas. Depending on the applied laser intensity, the optomechanical coupling of the membrane motion to transitions between two internal atomic states can be tuned. Above a critical intensity, a nonequilibrium quantum phase transition occurs to a symmetry-broken phase with a sizeable occupation of the energetically higher internal states and a displaced membrane. Its order can be changed by tuning the transition frequency. For symmetric coupling, it is continuous below a certain transition frequency and discontinuous above. For an asymmetric coupling, a first-order phase transition occurs.

Intriguing collective behavior emerges when different quantum many-body systems with complementary advantages are combined. In recently realized hybrids, state-of-the-art optomechanical systems are merged with atom-optical quantum systems in form of a cloud of  $^{87}\text{Rb}$  atoms into a single atom-optomechanical set-up. In this way, as theoretically proposed [1] and later experimentally realized [2–5], the vibrational motion of a nanomembrane in an optical cavity is coupled to the spatial motion of a distant cloud of cold  $^{87}\text{Rb}$  atoms that reside in the optical lattice of the out-coupled light field. In order to overcome the resolved sideband cooling limit and cool the nanomechanical oscillator close to its quantum mechanical ground state, the atom gas can be used as a coolant [1–4], collective effects in the quantum many-body system lead to collective atomic motion with an instability [5] and a continuous quantum phase transition [6] to a state with a spatially shifted optical lattice. Besides, investigations such as indirect measurement, a way to induce atom-membrane entanglement and coherent state transfer are in the focus of interest [7–11].

For a near resonant coupling mechanism, this motional coupling scheme limits the frequency of the nanooscillator to feasible trap frequencies in the optical lattice, which is in the sub-MHz regime. An eligible candidate to circumvent this problem is the so-called internal state coupling scheme [12] which allows a better tunability in order to reach a resonant coupling regime. Here, the mechanical motion of the membrane is indirectly coupled to transitions between internal states, e.g., Zeeman or hyperfine ground states, of the atomic gas via translating the phase shift of the light due to the membrane displacement into a polarization rotation using a polarizing beam splitter (PBS). This allows a near resonant coupling mechanism for membrane frequencies beyond the sub-MHz regime. Yet, a vast number of methods to perturb the internal states in the atom gas and influence the nanooscillator are applicable. These can be used to induce membrane cooling [12, 13], a displacement squeezed membrane [14], or to realize a harmonic oscillator with negative mass by the internal states [15].

On the other hand, the collective nature of the hybrid system mediates long-range interactions in the atom gas similar to those in a spinor dipolar Bose-Einstein condensate (BEC) [16, 17]. It is well known that long-range interactions in quantum gases induce long-range order and new phases of matter. A renowned hybrid quantum system includes an ultracold cloud of atoms inside a high finesse cavity that is transversely pumped by a laser [18, 19]. The collective coupling of the atoms to a single cavity mode induces long-range atom-atom interactions over the whole cavity. Above a critical interaction strength, this leads to a second-order nonequilibrium quantum phase transition (NQPT) to a self-organized superradiant state with a checkerboard pattern [18–22].

In this work, we investigate a hybrid atom-optomechanical system in the “membrane-in-the-middle-setup” [12]. The light field is adiabatically eliminated, leading to an effective coupling between the membrane and the transition between two states in the atom gas, see Fig. 1. In a mean-field description, the atomic part is reduced to a single-site problem with a Gaussian ansatz for the condensate profile. Tuning the atom-membrane coupling by alteration of the laser intensity, the system undergoes a NQPT. Moreover, we show that, by tuning the transition frequency, the order of the phase transition can be changed from second to first order and *vice versa*. In case of a discontinuous phase transition, the system exhibits a hysteresis which can be measured on the basis of polarization measurements of the atom gas.

## I. MODEL

We consider an ensemble of  $N$  ultracold  $^{87}\text{Rb}$  atoms placed in an external optical lattice. The atoms exhibit three relevant internal states  $\tau \in \{-, +, e\}$  that are arranged in a  $\Lambda$ -type level scheme. The two lowest states are energetically separated by  $\Omega_a$  which can be tuned via an external magnetic field ( $\hbar = 1$ ). A potential realization are the two hyperfine states  $|-\rangle = |F = 2, m_F = -2\rangle$  and  $|+\rangle = |F = 2, m_F = 0\rangle$  of the  $5^2S_{1/2}$  ground state.

The transition between  $|+\rangle$  and  $|e\rangle$  is driven by an applied  $\sigma_-$  circularly polarized laser with a finite detuning  $\Delta$ . The passing beam is directed to a PBS which divides the circularly polarized light into linearly polarized  $\pi_x$  and  $\pi_y$  light beams on two equal length arms (measured for an undisplaced membrane), see Fig. 1. The vertical path consists of a fixed mirror which reflects light with conserved polarization  $\pi_x$ . In the horizontal path, a nanomembrane is placed inside a low-finesse cavity, which reflects  $\pi_y \rightarrow \pi_y$  light when undisplaced. Here, a single vibrational mode of the membrane with frequency  $\Omega_m$  is considered. The outcoupled light of both arms is directed back onto the atoms mediating the effective atom-membrane coupling. In a quasi-static picture, a finite displacement of the membrane induces a finite phase shift on the propagating horizontal  $\pi_y$  beam leading to a rotated polarization after the light has passed the PBS backwards. The emergent  $\sigma_+$  photon with frequency  $\omega_+$  now impinges on an atom and may induce a two-photon transition between the states  $|-\rangle \leftrightarrow |+\rangle$ , when the resonance condition  $\Omega_m \simeq \Omega_a$  is met, such that  $\omega_+ = \omega_L + \Omega_a \simeq \omega_L + \Omega_m$ . The back-action of the atoms on the membrane is induced by a transition of the atoms between the states  $|\pm\rangle$ . The emitted  $\sigma_+$  photons pass the PBS with 50% probability horizontally and hit the membrane. This changes the radiation pressure on the membrane.

In the bad-cavity limit, the light field and  $|e\rangle$  can be eliminated in a Born-Markov approximation. In the mean-field regime, the hybrid atom-membrane system is effectively described by the equations of motion A

$$i\dot{\alpha} = (\Omega_m - i\Gamma_m)\alpha - \sqrt{N}\lambda_{\text{ex}} \int dz \cos(2z) |\psi_+|^2 - \sqrt{N}\lambda \int dz \cos(2z) \text{Re} \{ \psi_+^* \psi_- \}, \quad (1a)$$

$$i\dot{\psi}_- = \left[ N \sum_{\tau=\pm} g_{\tau-} |\psi_{\tau}|^2 - \frac{\Omega_a}{2} - \omega_R \partial_z^2 - \frac{V}{2} \cos(2z) \right] \psi_- - \sqrt{N}\lambda \text{Re}(\alpha) \cos(2z) \psi_+, \quad (1b)$$

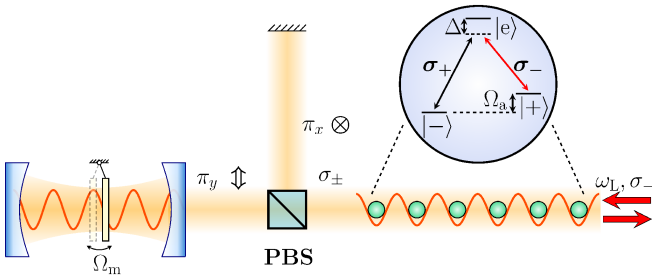


FIG. 1. Schematic sketch of the system. A nanomechanical membrane in an optical cavity is coupled to the internal states of a distant atom gas residing in an optical lattice potential.

$$i\dot{\psi}_+ = \left[ N \sum_{\tau=\pm} g_{\tau+} |\psi_{\tau}|^2 + \frac{\Omega_a}{2} - \omega_R \partial_z^2 - \frac{V}{2} \cos(2z) \right] \psi_+ - \text{Re}(\alpha) \cos(2z) \left[ \sqrt{N}\lambda \psi_- + 2\sqrt{N}\lambda_{\text{ex}} \psi_+ \right], \quad (1c)$$

with the first equation describing the motion of the membrane, and the latter two the motion of the two species condensate. Here,  $\alpha = \langle a \rangle / \sqrt{N}$  is the scaled mean value of the ladder operator  $a$  that annihilates an excitation on the membrane,  $\psi_{\pm}$  are the condensate wave functions of the corresponding internal state and  $N$  denotes the number of atoms. Fluctuations due to light field and thermal fluctuation are neglected. The atoms are placed in an optical lattice with depth  $V$  and local atom-atom interactions with strength  $g_{\tau\tau'}$  are included. Moreover,  $\omega_R = \omega_L^2 / 2m$  is the recoil frequency of the atoms with mass  $m$ . The atom-membrane coupling consists of two different processes. First, the coupling induces transitions between the internal states  $\tau = -$  and  $\tau = +$  with coupling constant  $\lambda$ . Second, a term arises which couples the occupation number of atoms in the state  $\tau = +$  to the membrane displacement with strength  $\lambda_{\text{ex}}$  [6]. In fact, the coupling constants are not independent of each other as  $\lambda_{\text{ex}} / \lambda = 2\mu_+ / \mu_- = \chi / 2$ , where  $\mu_{\tau}$  is the atomic transition dipole moment for the corresponding internal state. Hence, we choose the parametrization  $\lambda_{\text{ex}} = \chi \lambda / 2$  and refer to the case  $\chi = 0$  as symmetric coupling.

For a deep optical lattice,  $V \gg \omega_R$ , the condensate profile is well described by a sum of Gaussians residing in the individual lattice wells. When the wave function overlap between neighboring sites is small, the problem reduces to a single-site problem. It is then reasonable to make the ansatz

$$\psi_{\tau}(t, z) = c_{\tau}(t) \left[ \frac{1}{\pi\sigma(t)^2} \right]^{1/4} e^{-z^2/2\sigma(t)^2 + i\beta(t)z^2}, \quad (2)$$

with a constant number of atoms, i.e.,  $|c_-|^2 + |c_+|^2 = 1$ , the condensate width  $\sigma$ , and  $\beta$  is used to produce the dynamics for  $\sigma$ . For a binary BEC, the ground state is either in a miscible or immiscible state, where the condensate profile of the different internal states are either mixable or avoid each other. This feature depends on the ratio of the coupling constants  $\eta = g_{++}g_{--}/g_{+-}^2$ . The condensate is mixable for  $\eta > 1$  and non-mixable for  $\eta < 1$  [23, 24]. Moreover, it has been shown that a transition from an immiscible to a miscible state is induced by a linear interconversion coupling [25] which is similar to the present internal state coupling. For simplicity, we assume that the width is the same for both particle species and restrict this work to the case  $g_{\tau\tau'} \equiv g$ , i.e.,  $\eta = 1$ . The validity of this ansatz is verified by numerical estimations of the condensate profile B.

Next, we perform a cumulant expansion [6] of the Eqs. (1) to find the equations of motion for the respective variational parameters in Eq. (2). That is, we calculate the (i) 0<sup>th</sup> and (ii) 2<sup>nd</sup> cumulants by multiplying Eqs. (1b) and (1c) (i) with  $\psi_0(z) = (\pi\sigma^2)^{-1/4} e^{-z^2/2\sigma^2 - i\beta z^2}$  as well

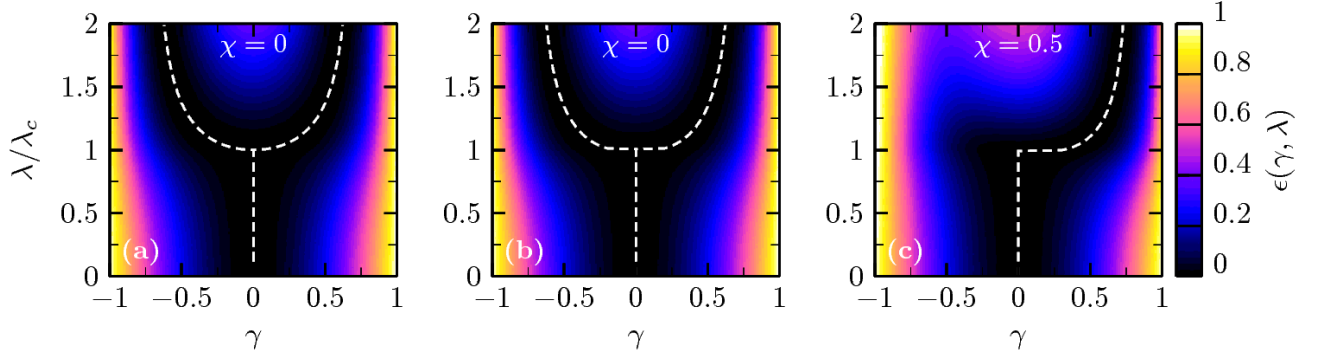


FIG. 2. Normalized potential energy surface  $\epsilon(\gamma, \lambda)$  as a function of the atomic polarization parameter  $\gamma$  and the atom-membrane coupling  $\lambda$ . (a) and (b) represent the symmetric case ( $\chi = 0$ ) with  $\Omega_a = 50 \omega_R$  and  $\Omega_a = 5000 \omega_R$ , respectively. In (a), the system shows a second-order phase transition, whereas the system undergoes a first-order phase transition in (b). (c) In the regime of non-symmetric coupling  $\chi \neq 0$  (here,  $\chi = 0.5$  and  $\Omega_a = 50 \omega_R$ ), the system exhibits always a first-order phase transition above a critical coupling rate, where only one branch corresponds to the energetically lowest steady state, while the other branch is energetically raised. Other parameters are  $V = 100 \omega_R$ ,  $\Omega_m = 2 \Omega_a$ ,  $\Gamma_m = 0.1 \Omega_m$  and  $gN = \omega_R$ .

as (ii) with  $(z^2 - \sigma^2/2)\psi_0(z)$  and integrate then over  $z$ . This leads to five independent equations of motions of which one is  $\dot{\sigma} = 4\omega_R\beta\sigma$ , and

$$\begin{aligned}\dot{\alpha} &= -i\partial_{\alpha^*}E - \Gamma_m\alpha, \\ \dot{c}_\tau &= -i\partial_{c_\tau^*}E, \\ (4\omega_R)^{-1}\ddot{\sigma} &= -\partial_\sigma E,\end{aligned}\quad (3)$$

with the effective potential energy

$$\begin{aligned}E &= \Omega_m|\alpha|^2 + \frac{\Omega_a}{2} [|c_+|^2 - |c_-|^2] + \left[ \frac{\omega_R}{2\sigma^2} + \frac{Ng}{\sqrt{8\pi}\sigma} \right. \\ &\quad \left. - \frac{V}{2e\sigma^2} \right] - \sqrt{N}\lambda [\chi|c_+|^2 + 2\text{Re}(c_+^*c_-)] \frac{\text{Re}(\alpha)}{e\sigma^2}.\end{aligned}\quad (4)$$

## II. TUNING THE ORDER OF THE QUANTUM PHASE TRANSITION

In the presence of damping, the system will eventually relax to a steady state. Thus, each of the parameters can be split into their steady state value and deviations from the steady state. Here, we are mainly interested in the steady state properties of the combined hybrid system. That is, we make the ansatz  $\alpha(t) = \alpha_0$ ,  $c_-(t) = \sqrt{1 - \gamma_0^2}$ ,  $c_+(t) = \gamma_0$ ,  $\sigma(t) = \sigma_0$ . By inserting this ansatz in Eq. (3), the relation  $\alpha_0 = \sqrt{N}\lambda[2\gamma_0\sqrt{1 - \gamma_0^2} + \chi\gamma_0^2]e^{-\sigma_0^2}/2(\Omega_m - i\Gamma_m)$  is found, whereas the condensate parameters  $\gamma_0$ ,  $\sigma_0$  are determined via  $\Omega_a\gamma_0\sqrt{1 - \gamma_0^2} = \sqrt{N}\lambda\text{Re}(\alpha_0)e^{-\sigma_0^2}[1 - 2\gamma_0^2 + \chi\gamma_0\sqrt{1 - \gamma_0^2}]$ , and  $\omega_R + gN\sigma_0/\sqrt{8\pi} = [V + 2\sqrt{N}\lambda\text{Re}(\alpha_0)(2\gamma_0\sqrt{1 - \gamma_0^2} + \chi\gamma_0^2)]e^{-\sigma_0^2}\sigma_0^4$ .

For a qualitative understanding of the role of both the atom-membrane coupling  $\lambda$  and the asymmetry  $\chi$ , we study the potential energy surface in Eq. (4). The optimal choice of parameters  $(\alpha_0, \gamma_0, \sigma_0)$  is characterized by a globally minimized potential energy  $E_{\min} =$

$E[\alpha_0, \gamma_0, \sigma_0]$  (note that  $\alpha_0$  is fixed by  $\gamma_0$  and  $\sigma_0$ ). Rather than minimizing the energy potential with respect to all three parameters, we minimize with respect to  $\alpha_0$ ,  $\sigma_0$  for a given  $\gamma$ , which is taken as an order parameter, and study the resulting potential energy surface  $E(\gamma) = E[\alpha_0(\gamma), \gamma, \sigma_0(\gamma)]$ . The global symmetry properties of the hybrid system are determined by  $\gamma$  via the influence of the occupations of the condensate species ( $c_+(t) = \gamma$ ,  $c_-(t) = \sqrt{1 - \gamma^2}$ ).

Figure 2 shows the normalized energy surface  $\epsilon(\gamma, \lambda) = [E(\gamma) - E(0)]/\max_{|\gamma| \leq 1} \{E(\gamma) - E(0)\}$ . The dashed curves show the value  $\gamma_0$  that minimizes the energy potential. Below a certain coupling rate  $\lambda \leq \lambda_c$ , the potential is minimized for  $\gamma_0 = 0$  in which all atoms occupy the state  $|\tau = -\rangle$ . At  $\lambda = \lambda_c$ , the system undergoes a NQPT that is characterized by a non-vanishing  $\gamma_0 \neq 0$  with different characteristics. The case  $\chi = 0$  is shown in Fig. 2(a) and (b). In Fig. 2(a), the NQPT is of second order with a critical exponent  $\gamma_0 \sim (\lambda - \lambda_c)^{1/2}$ . By tuning the transition frequency  $\Omega_a$ , the NQPT becomes a symmetric first-order phase transition, see Fig. 2(b). Here, the bistable phase corresponds to the two states  $(|-\rangle \pm |+\rangle)/\sqrt{2}$ . For a non-vanishing asymmetry  $\chi > 0$ , an asymmetric first-order phase transition occurs at the critical coupling, where the left branch  $(|-\rangle - |+\rangle)/\sqrt{2}$  is energetically raised, see Fig. 2(c).

In order to quantify which type of NQPT occurs and to specify the critical coupling rate, we perform a Landau expansion of the potential energy  $E(\gamma) = \sum_{n \geq 2} a_n \gamma^n$  in the order parameter around  $\gamma = 0$ . For symmetric coupling  $\chi = 0$ , only even orders in  $\gamma$  turn out to contribute and the critical coupling rate for the second-order NQPT  $\lambda_{s2}$  is defined by  $a_2 = 0$ , whereas critical coupling for the symmetric first-order NQPT  $\lambda_{s1}$  is approximately estimated via  $13a_2a_6 = 4a_4^2$ . Moreover, the order of the NQPT is determined by the modulus of  $a_4$ . At the point  $a_4 = 0$ , a transition from a second- to a symmetric first-

order NQPT occurs, which allows us to define a critical transition frequency

$$\Omega_c = \frac{\omega_\sigma^2}{32\omega_R\sigma_0^2}, \quad (5)$$

where  $\omega_\sigma^2 = 4\omega_R[3\omega_R/\sigma_0^4 + Ng/\sqrt{2\pi}\sigma_0^3 + V(1-2\sigma_0^2)e^{-\sigma_0^2}]$  is the frequency of the condensate breathing mode. For  $\Omega_a < \Omega_c$ , the NQPT is continuous, whereas it becomes discontinuous for  $\Omega_a > \Omega_c$ . This fact is shown in Fig. 3 as a function of the lattice depth  $V$  in (a) and the interaction strength  $gN$  in (b). The asymmetric coupling  $\chi \neq 0$  gives rise to terms of odd order in  $\gamma$  in the Landau expansion and the NQPT is always discontinuous. Here, the critical coupling  $\lambda_c = \lambda_{a1}$  is approximated by the smallest solution for  $\lambda$  of the equation  $4a_2a_4 = a_3^2$ . By expanding the defining equations, it follows that  $\lambda_{a1}, \lambda_{s1} < \lambda_{s2}$ .

### III. HYSTERESIS

A characteristic feature of a first-order phase transition is the occurrence of hysteresis, shown in Fig. 4(a) and (b) for  $\chi = 0$  and  $\chi = 0.5$ , respectively. To obtain hysteresis, we take the equations of motion (3) with  $\gamma(t) = c_+(t)$ , in the limit of infinite time, i.e.,  $\lim_{t \rightarrow \infty} \gamma(t) = \gamma_\infty$ . On the forward path, the coupling strength  $\lambda$  is adiabatically increased and the system is initially placed in the minimum at  $\gamma = 0$ . The system stays there until it becomes unstable at  $\lambda = \lambda_f$  and jumps to the adjacent minimum at  $\gamma_0 \neq 0$ . This point is defined by  $a_2 = 0$  and coincides with the critical coupling rate  $\lambda_{s2}$  in the symmetric regime. Afterwards, the steady state solution  $\gamma_0$  is followed as  $\lambda$  increases.

On the backward path, the system follows the minimum at  $\gamma_\infty \neq 0$  until this point becomes unstable at  $\lambda_b$  and jumps to the solution at  $\gamma_\infty = 0$ . For the symmetric case (a), this jumping point is given by the relation  $3a_2a_6 - a_4^2 = 0$ , whereas it is given by the relation  $9a_3^2 - 32a_2a_4 = 0$  for the asymmetric case (b).

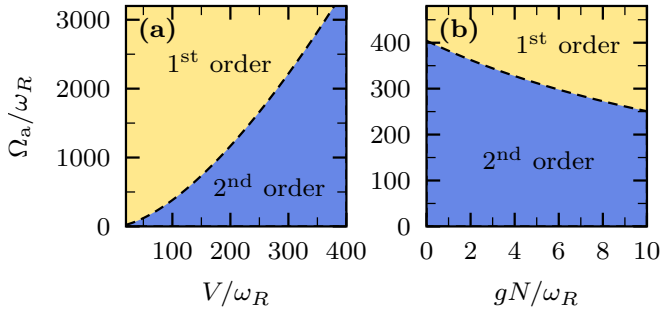


FIG. 3. Order of the NQPT as a function of the atomic transition frequency  $\Omega_a$  and (a) the lattice depth  $V$  or (b) the interaction strength  $gN$ . The dashed lines show the critical transition frequency  $\Omega_a = \Omega_c$  according to Eq. (5). The fixed parameter in (a) is the interaction strength  $gN = \omega_R$  and in (b) the potential depth  $V = 100\omega_R$ .

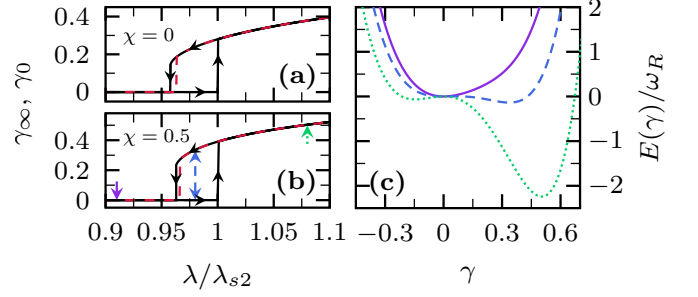


FIG. 4. Hysteresis and potential curves. Hysteresis curve ( $\gamma_\infty$ , solid) as a function of the coupling parameter  $\lambda$  for (a) the symmetric 1st order ( $\chi = 0$ ) and (b) the asymmetric 1st order PT ( $\chi = 0.5$ ). The dashed line shows the stationary order parameter  $\gamma_0$ . (c) Potential curves for different coupling strengths as indicated by the arrows in (b). Parameters chosen for (a) as in Fig. 2(b) and for (b), (c) as in Fig. 2(c).

In the picture of potential energy surfaces, the reason of the hysteresis behavior is the existence two stable local minima at  $\gamma = 0$  and  $\gamma \neq 0$  in the coexistence region  $\lambda_b \leq \lambda \leq \lambda_f$  as indicated in Fig. 4(c) for  $\chi = 0.5$ .

### IV. EXPERIMENTAL REALIZATION

An experimental realization of the discussed coupling scheme has not yet been established. Current experimental set-ups use the motional coupling scheme [1, 2]. This system also exhibits a NQPT from a localized symmetric state to a symmetry-broken quantum many-body state with a shifted cloud-membrane configuration [6]. Here, the relevant energy scale of the condensate, which corresponds to the breathing mode frequency, is the energy to excite particles to a higher motional band, see Eq. (5). Both of these frequencies scale with the lattice depth, which makes a direct observation of the transition from a second- to a first-order NQPT impossible. This considerably improves for the internal state coupling scheme as considered here. For the proposed system, the direct observation is possible by either measuring the membrane eigenfrequency or the condensate width  $\sigma_0$  [6]. In the case of a first-order NQPT, these quantities exhibit a jump at the critical coupling rate, rather than a continuous behavior as in the case of a second-order NQPT. Moreover, a direct measurement of the condensate polarization  $\gamma_0$  ( $\gamma_\infty$ ) can detect the NQPT in a straightforward way. Furthermore, the asymmetry parameter  $\chi$  can be tuned by applying an additional perpendicular laser field that drives the transition from  $|-\rangle$  to  $|+\rangle$ , giving rise to a term  $\delta(c_+^*c_- + c_+^*c_-)$  in the potential energy (4). Compensating an additional force on the membrane that scales with  $\sqrt{N}\lambda$  and tuning the parameter  $\delta$  allows an indirect variation of the asymmetry parameter  $\chi$ .



## V. CONCLUSION

We have shown that the hybrid atom-optomechanical system not only undergoes a nonequilibrium quantum phase transition between phases of different collective behavior, but also that the order of the phase transition can be tuned in a straightforward manner. The steady state of an ultracold atomic condensate in an optical lattice, whose internal states are coupled to a single mechanical vibrational mode of a distant membrane, has been analyzed, based on a Gross-Pitaevskii-like mean-field approach by a time-dependent Gaussian variational ansatz. Mediated by the light field of a common laser, the coupling between the atoms and the membrane is tuned by changing the laser intensity. Below a certain critical coupling  $\lambda_c$ , all the atoms occupy the energetically lower state  $|-\rangle$  and at the critical point a nonequilibrium quantum phase transition occurs. This phase is characterized by a sizeable steady-state occupation of the energetically higher state  $|+\rangle$  and a displaced membrane. Its order is determined by the state-dependent atom-membrane coupling and the transition frequency  $\Omega_a$ . For an asymmetric coupling,  $\chi \neq 0$ , an asymmetric first-order phase transition occurs with a preferred polarization orientation. Instead, for a symmetric coupling,  $\chi = 0$ , the phase transition is continuous for transition frequencies below a certain critical value  $\Omega_c$  and discontinuous above. Moreover, hysteresis is obtained by adiabatically tuning the coupling strength in the regime of a first-order phase transition. The transition between a first- and second-order is observable by tuning readily accessible parameters in the internal state coupling scheme.

## ACKNOWLEDGEMENTS

This work was supported by the Deutsche Forschungsgemeinschaft (N.M.) and the DFG Collaborative Research Center/TransRegio 185 "Open System Control of Atomic and Photonic Matter" (A.P.).

### Appendix A: Effective Hamiltonian of the Hybrid System

In order to obtain an effective Hamiltonian of the hybrid system, we start from the total system Hamiltonian consisting of five parts, i.e.,

$$H_{\text{tot}} = H_m + H_a + H_l + H_{m-l} + H_{a-l}. \quad (\text{A1})$$

Each of the first three terms describes one of the three compounds: the nanomembrane, the atomic condensate and the light field, respectively. The coupling between the light field and the membrane or the atoms is described by the last two terms. The nanomembrane is modeled as a single vibrational mode with ( $\hbar = 1$ )

$$H_m = \Omega_m b^\dagger b. \quad (\text{A2})$$

The atomic part is a condensate of bosonic atoms which have three relevant internal states represented by the bosonic field operators  $\Psi_\tau(z)$  with  $\tau \in \{-, +, e\}$ . The Hamiltonian is given by

$$H_a = \sum_\tau \int dz \Psi_\tau^\dagger \left[ V_\tau(z) - \omega_R \partial_z^2 + \sum_{\tau'} \frac{g_{\tau\tau'}}{2} \Psi_{\tau'}^\dagger \Psi_{\tau'} \right] \Psi_\tau. \quad (\text{A3})$$

Here,  $\omega_R = \omega_L^2/2m$  is the recoil frequency with the laser frequency  $\omega_L$  and the mass  $m$  of the atoms. Moreover, we assume a contact interaction and the one-dimensional interaction strength between two atoms with internal states  $\tau$  and  $\tau'$  is  $g_{\tau\tau'}$ . The potential  $V_\tau(z)$  includes the energy of the corresponding internal state and an optical lattice potential for the external spatial degree of freedom of the atoms. The three internal atomic states are energetically arranged as shown in Fig. 1 in the main paper. The light modes have two possible optical polarizations which are described by the operators  $a_\omega, b_\omega$  and included over a bandwidth  $2\theta$  around  $\omega_L$ . They are described by

$$H_l = \int_{\omega_L - \theta}^{\omega_L + \theta} d\omega \Delta_\omega [a_\omega^\dagger a_\omega + b_\omega^\dagger b_\omega], \quad (\text{A4})$$

with  $\Delta_\omega = \omega - \omega_L$ . All of the above defined operators fulfill bosonic commutation relations.

An external laser with field strength  $\alpha_L$  and circular polarization  $\sigma_-$  is included by the linear replacement

$$a_\omega \rightarrow a_\omega + \delta(\omega - \omega_L) e^{-i\omega_L t} \alpha_L, \quad (\text{A5})$$

such that the coupling between the light field and the membrane (atoms) can be linearized in  $a_\omega$  and  $b_\omega$ . In a reference frame that rotates with the laser frequency, the linearized membrane-light field interaction takes the form

$$H_{m-l} = \lambda_m (a + a^\dagger) \int \frac{d\omega}{\sqrt{2\pi}} (a_\omega + a_\omega^\dagger + b_\omega + b_\omega^\dagger), \quad (\text{A6})$$

with the coupling strength  $\lambda_m$ . In the "membrane-in-the-middle" set-up, the membrane-light field coupling scales as [1]

$$\lambda_m = \frac{\alpha_L |r_m| \omega_L}{\sqrt{\Omega_m M}} \frac{2\mathcal{F}}{\pi^{3/2}}, \quad (\text{A7})$$

with the membrane reflectivity  $|r_m|$ , membrane mass  $M$  and cavity finesse  $\mathcal{F}$ .

After elimination of the auxiliary state  $\sigma = e$ , the atom-light field coupling

$$H_{a-l} = \int \frac{d\omega}{\sqrt{2\pi}} \int dz \sin(z) \sin(\frac{\omega}{\omega_L} z) \left[ \lambda_- b_\omega \Psi_+^\dagger(z) \Psi_-(z) + \lambda_- b_\omega^\dagger \Psi_-(z) \Psi_+(z) + \lambda_+ (a_\omega + a_\omega^\dagger) \Psi_+^\dagger(z) \Psi_+(z) \right] \quad (\text{A8})$$

consists of several terms describing different effects. The first two terms in the square bracket lead to transitions

between the atomic internal states under the creation (or annihilation) of a polarized photon. On the other hand, the last term couples the atoms in the internal state  $\tau = +$  to the photon field quadrature, in a similar manner as in a motional coupling scheme [1]. Here, the atom-light coupling constants are given by [12]

$$\lambda_\tau = \sqrt{\frac{2}{\pi}} \alpha_L \omega_L \frac{\mu_+ \mu_\tau}{\mathcal{A} \Delta}, \quad (\text{A9})$$

with the beam cross-sectional area  $\mathcal{A}$ , the dipole moments  $\mu_\tau$  of the atoms in the corresponding internal state  $\tau$  and the light field detuning  $\Delta$ , see also Fig. 1 of the main paper. In order to obtain an effective description that includes the atom-membrane coupling directly, we adiabatically eliminate the light modes. We start with the linearized Hamiltonian (A1) in the interaction picture with respect to  $U(t) = \exp\{iH_I t\}$ . The formal solution of the Schrödinger equation in the interaction picture reads

$$|\psi(t)_I\rangle = \mathcal{T} \exp\left\{-i \int_0^t dt' H'(t')_I\right\} |\psi(0)\rangle, \quad (\text{A10})$$

with the time-ordering operator  $\mathcal{T}$ , the index  $I$  indicating the interaction picture and  $H' = H_{\text{tot}} - H_I$ . Next, we expand the right-hand side for small time increments  $\delta t$ . Up to second order, the relevant terms read

$$|\psi(\delta t)_I\rangle \simeq \left\{1 - i \int_0^{\delta t} dt H'(t)_I - \int_0^{\delta t} dt \int_0^t dt' H'(t)_I H'(t')_I\right\} |\psi(0)\rangle. \quad (\text{A11})$$

Moreover, we assume that the initial state is a product state  $|\psi(0)\rangle = |\psi\rangle_{\text{a+m}} \otimes |\text{vac}\rangle_1$ , where  $|\text{vac}\rangle_1$  is the vacuum state of the light field and  $|\psi\rangle_{\text{a+m}}$  is an arbitrary state in the atom-membrane subspace. Hence, we assume  $a_\omega |\psi(0)\rangle = b_\omega |\psi(0)\rangle = 0$  and define the noise-increment operators

$$\delta A(t) = \int_t^{t+\delta t} ds \int \frac{d\omega}{\sqrt{2\pi}} a_\omega(s)_I, \quad (\text{A12})$$

$$\delta B(t) = \int_t^{t+\delta t} ds \int \frac{d\omega}{\sqrt{2\pi}} b_\omega(s)_I, \quad (\text{A13})$$

$$\delta C(t) = \int_t^{t+\delta t} ds \int \frac{d\omega}{\sqrt{2\pi}} \sin(\frac{\omega}{\omega_L} z) b_\omega(s)_I. \quad (\text{A14})$$

Next, we take the limit  $\delta t \rightarrow 0$  and assume that the noise-increment operators after a time step  $\delta t$  do not depend on their form at the earlier time, which is equivalent to the Markov approximation. Then, we can derive a quantum stochastic Schrödinger equation in the Ito form with  $d|\psi(t)\rangle = |\psi(t+dt)\rangle - |\psi(t)\rangle$ . The differential noise operators, e.g.,  $\delta A(t) \rightarrow_{\delta t \rightarrow 0} dA(t)$ , follow the Ito rules

$$dA(t)dA^\dagger(t) = dB(t)dB^\dagger(t) = dt, \quad (\text{A15})$$

$$dB(t)dC^\dagger(t) = dC(t)dB^\dagger(t) = \sin(z)dt, \quad (\text{A16})$$

$$dC(t)dC^\dagger(t) = \sin(z)\sin(z')dt. \quad (\text{A17})$$

With these relations, the effective equations of motion for the reduced system can be derived in the form

$$i\dot{a} = [\Omega_m - i\Gamma_m]a - \lambda_{\text{ex}} \int dz \cos(2z) \Psi_+^\dagger \Psi_+ - \frac{\lambda}{2} \int dz \cos(2z) [\Psi_-^\dagger \Psi_+ + \Psi_+^\dagger \Psi_-], \quad (\text{A18})$$

$$i\dot{\Psi}_- = \left[ \sum_\tau g_{\tau-} \Psi_\tau^\dagger \Psi_\tau - \frac{\Omega_a}{2} - \omega_R \partial_z^2 - \frac{V}{2} \cos(2z) \right] \Psi_- - \frac{\lambda}{2} (a + a^\dagger) \cos(2z) \Psi_+$$

$$i\dot{\Psi}_+ = \left[ \sum_\tau g_{\tau+} \Psi_\tau^\dagger \Psi_\tau + \frac{\Omega_a}{2} - \omega_R \partial_z^2 - \frac{V}{2} \cos(2z) \right] \Psi_+ - \frac{\lambda}{2} (a + a^\dagger) \cos(2z) \Psi_- - \lambda_{\text{ex}} (a + a^\dagger) \cos(2z) \Psi_+, \quad (\text{A19})$$

where we have inserted the potential  $V_\tau(z) = \tau\Omega_a/2 - V\cos(2z)/2$ . Moreover, we have neglected terms which are introduced by the light field and lead to long-range interaction in the atomic condensate. This assumption is justified if the laser frequency is far detuned from the transition frequency between the states  $\tau = +$  and  $\tau = e$ . Furthermore, we have defined the coupling constants  $\lambda = \lambda_- \lambda_m/4$  and  $\lambda_{\text{ex}} = \lambda_+ \lambda_m/2$ . Finally, fluctuations introduced by the light field have been neglected and a phenomenological damping of the membrane mode with rate  $\Gamma_m$  has been introduced.

The equations of motion of the coupled system of Eq. (1) in the main text are obtained in the condensate regime. Then, a large fraction of atoms occupy the ground state. Assuming weak atom-atom interaction and atom-membrane coupling, i.e.,  $g_{\tau\tau'}, \lambda, \lambda_{\text{ex}} \ll \omega_R, \Omega_m$ , the field operators can be approximated by complex functions  $\Psi_\tau(z) \simeq \sqrt{N} \psi_\tau(z)$ . Likewise, the mechanical ladder operator can be approximated by its mean value  $a \simeq \langle a \rangle = \sqrt{N} \alpha$ .

## Appendix B: Immiscible and miscible Phase

A binary BEC is either in a miscible or immiscible phase which is characterized by a formation or absence of a homogeneous mixture, respectively. In other words, the overlap between the wave functions  $\psi_\pm(z)$  is minimized in the immiscible phase. The value  $\eta = g_{--}g_{++}/g_{+-}^2$  determines whether the condensate is mixable ( $\eta > 1$ ) or not ( $\eta < 1$ ) [23, 24]. In this work, we consider  $g_{--} = g_{++} = g_{+-}$  with  $\eta = 1$  which is just at the boundary between miscibility and immiscibility.

To justify our ansatz in Eq. (2), we estimate the steady state condensate profile of the extended Gross-Pitaevskii equation (GPE), see Eq. (1) of the main text. In Fig. 5, the condensate profile in a single potential well is shown

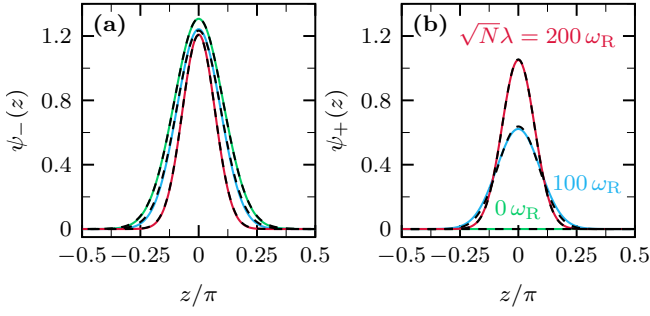


FIG. 5. Condensate wave function for different atom-membrane coupling constants for symmetric coupling  $\chi = 0$ . The solid curves show the results from the Gaussian variational ansatz and the dashed curves show the numerical result obtain from the GPE. The condensate profile for the internal states  $\tau = -$  and  $\tau = +$  are shown in the panels (a) and (b), respectively. Other parameters used are  $V = 100 \omega_R$ ,  $gN = \omega_R$ ,  $\Omega_a = 50 \omega_R$ ,  $\Omega_m = 100 \omega_R$ , and  $\Gamma_m = 10 \omega_R$ .

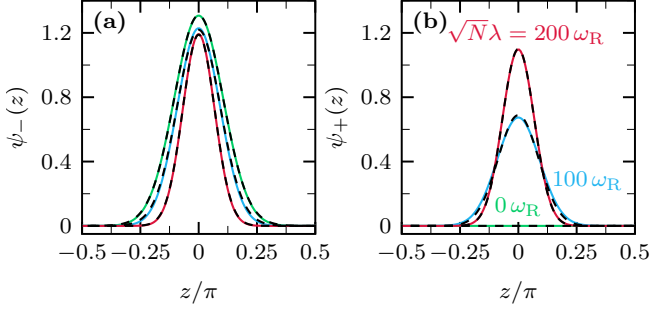


FIG. 6. Same as in Fig. 5, but for the asymmetric coupling regime with  $\chi = 0.1$ .

for the case  $\chi = 0$  and different coupling constants  $\lambda$ . The panels (a) and (b) show the condensate profile of the internal state  $\tau = -$  and  $\tau = +$ , respectively, as a function of the position  $z$ . The well minimum is located at  $z = \pi/4$ . Different colors translate to different coupling constants, as indicated in Fig. 5 (b). Moreover, the solid curves show the semi-analytical Gaussian ansatz, whereas the dashed curves show the full numerical result of the GPE with the respective coupling constants being non-zero. Overall, a good agreement for the condensate wave function between the semi-analytical and numerical results is found. Only slight deviations in the vicinity of the phase transition are found, which are here indicated by the blue result in Fig. 5(b).

Considering a small asymmetry in the coupling (here  $\chi = 0.1$ ), the Gaussian ansatz with a state independent condensate width  $\sigma_0$  is in good agreement with the numerically calculated steady state condensate profile. This scenario is shown in Fig. 6.

### Appendix C: Landau Expansion of the Nonequilibrium Potential

In order to quantify the type of the nonequilibrium quantum phase transition (NQPT), i.e., whether a first or second order quantum phase transition occurs, we expand the nonequilibrium potential  $E(\alpha, \gamma, \sigma)$  in terms of the order parameter  $\gamma$  around  $\gamma_0 = 0$ . In general, the Taylor expansion takes the form  $E(\gamma) = \sum_{n \geq 2} a_n \gamma^n + a_0$ . With the relation  $\alpha_0 = \sqrt{N} \lambda [2\gamma \sqrt{1 - \gamma^2} + \chi \gamma^2] e^{-\sigma_0^2/2} / (\Omega_m - i\Gamma_m)$ , the potential reduces

$$E = -\frac{\Omega_a}{2} [1 - 2\gamma^2] - \frac{N\lambda^2}{4\Omega'_m} \left[ 2\gamma \sqrt{1 - \gamma^2} + \chi \gamma^2 \right]^2 e^{-2\sigma_0^2} + \frac{\omega_R}{2\sigma_0} + \frac{Ng}{\sqrt{8\pi}\sigma_0} - \frac{V}{2} e^{-\sigma_0^2}, \quad (C1)$$

with  $\Omega'_m = \Omega_m + \Gamma_m^2/\Omega_m$ . Moreover, the extremization parameter  $\sigma_0$  is implicitly defined via the relation  $F[\gamma, \sigma_0(\gamma)] = 0$  with the function

$$F[\gamma, \sigma] = \frac{\omega_R}{\sigma^3} + \frac{Ng}{\sqrt{8\pi}\sigma^2} - V\sigma e^{-\sigma^2} - \frac{N\lambda^2}{\Omega'_m} \left[ 2\gamma \sqrt{1 - \gamma^2} + \chi \gamma^2 \right]^2 \sigma e^{-\sigma^2}. \quad (C2)$$

By means of the theorem of implicit functions, the first derivative of the steady state width  $\sigma_0$  with respect to the order parameter  $\gamma$  is given by  $\sigma'_0 = (\partial \sigma_0 / \partial \gamma)|_{\gamma=0} = -(\partial_\gamma F[\gamma, \sigma]) / (\partial_\sigma F[\gamma, \sigma])|_{\sigma=\sigma_0, \gamma=0}$ . With this in mind, we find the implicit derivatives  $\sigma'_0 = 0$ ,  $\sigma''_0 = 3\chi \sigma'_0$ ,

$$\sigma''_0 = -8 \left( \frac{4\omega_R}{\omega_\sigma^2} \right) \frac{N\lambda^2}{\Omega'_m} \sigma_0 e^{-2\sigma_0^2}, \quad (C3)$$

$$\sigma_0^{(4)} = \frac{3 - 12\sigma_0^2}{\sigma_0} (\sigma_0'')^2 - (12 - 3\chi^2) \sigma_0'', \quad (C4)$$

where we have defined the frequency of the atomic breathing mode as

$$\omega_\sigma^2 = 4\omega_R \left[ \frac{3\omega_R}{\sigma_0^4} + \frac{Ng}{\sqrt{2\pi}\sigma_0^3} + V(1 - 2\sigma_0^2) e^{-\sigma_0^2} \right]. \quad (C5)$$

Without loss of generality, we can choose the Landau coefficient  $a_0 = 0$  by shifting the zero-point energy. The first Landau coefficient  $a_1$  is always zero and the second Landau coefficient is given by

$$a_2 = 2\Omega_a - 2 \frac{N\lambda^2}{\Omega'_m} e^{-2\sigma_0^2}. \quad (C6)$$

In the case of a second order NQPT,  $a_2 = a_2(\lambda_{s2}) = 0$  defines the critical coupling rate  $\lambda_{s2}$ , which can be reduced to the implicit equation

$$\omega_R + \frac{Ng}{\sqrt{8\pi}} \sqrt{\ln \frac{\lambda_{s2}}{\lambda_\Omega}} = V \left( \frac{\lambda_\Omega}{\lambda_{s2}} \right) \left( \ln \frac{\lambda_{s2}}{\lambda_\Omega} \right)^2, \quad (C7)$$

with the shorthand notation  $\sqrt{N}\lambda_\Omega = \sqrt{\Omega_a\Omega'_m}$ . In a more compact definition, the second Landau coefficient may be rewritten as  $a_2 = \Omega_a(1 - \lambda^2/\lambda_{s2}^2)$ . Moreover, the Landau coefficients up to sixth order read

$$a_3 = -\Omega_a \left( \frac{\lambda}{\lambda_{s2}} \right)^2 \chi, \quad (\text{C8})$$

$$a_4 = \Omega_a \left( \frac{\lambda}{\lambda_{s2}} \right)^2 \left[ 1 + \sigma_0 \sigma_0'' - \frac{\chi^2}{4} \right], \quad (\text{C9})$$

$$a_5 = \frac{\Omega_a}{2} \left( \frac{\lambda}{\lambda_{s2}} \right)^2 [1 + 4\sigma_0 \sigma_0''] \chi, \quad (\text{C10})$$

$$a_6 = \frac{\Omega_a}{6} \left( \frac{\lambda}{\lambda_{s2}} \right)^2 \left[ (1 - 4\sigma_0^2)(\sigma_0'')^2 - 3\sigma_0(4 - 3\chi^2)\sigma_0'' \right]. \quad (\text{C11})$$

Note that  $a_6$  is always positive since  $\sigma_0'' < 0$ . Consequently, it is sufficient to consider the Landau expansion up to sixth order.

### 1. Symmetric Coupling $\chi = 0$

In the symmetric coupling regime, the odd Landau coefficients vanish, since  $a_{2n+1} \sim \chi$ , and the Landau expansion takes the form

$$E(\gamma) = a_2\gamma^2 + a_4\gamma^4 + a_6\gamma^6 + \mathcal{O}(\gamma^8). \quad (\text{C12})$$

The order of the phase transition is determined by the sign of the expansion coefficient  $a_4$ . The phase transition is continuous for  $a_4 > 0$  and discontinuous for  $a_4 < 0$ . Indeed, the coefficient exhibits a point at which it changes its sign. This point is given by the relation  $1 + \sigma_0 \sigma_0'' = 0$ . For  $a_4 \geq 0$ , the phase transition occurs for  $a_2 = 0$  and we can express the coupling constant in terms of the atomic transition frequency  $\Omega_a$  to find the relation Eq. (5) in the main paper. By choosing the atomic transition frequency

$\Omega_a$  below the critical frequency  $\Omega_c$ , a second order NQPT occurs at the critical coupling constant defined by  $a_2 = 0$ .

If  $\Omega_a > \Omega_c$ , a first order NQPT occurs and the critical coupling constant can only be defined approximately. Therefore, we take the Landau expansion up to sixth order and estimate the local minima given by

$$\gamma_1 = 0 \vee \gamma_{2,3}^2 = -\frac{a_4}{3a_6} + \sqrt{\left( \frac{a_4}{3a_6} \right)^2 - \frac{a_2}{3a_6}}, \quad (\text{C13})$$

which are local minima only if  $a_2 > 0$ . Due to the definition of the potential, the minimum at  $\gamma_1$  is always at  $E(0) = 0$ . The critical coupling constant is found by equating  $E(\gamma_{2,3})|_{\lambda=\lambda_{s1}} = 0$ . After some tedious algebra, the relation

$$13a_2a_6 - 4a_4^2|_{\lambda=\lambda_{s1}} = 0 \quad (\text{C14})$$

is found.

### 2. Asymmetric Coupling $\chi \neq 0$

In a similar fashion, the critical coupling constant  $\lambda_{a1}$  can be estimated in the asymmetric coupling regime. Assuming that  $a_4 > 0$ , the Landau expansion is given by

$$E(\gamma) = a_2\gamma^2 + a_3\gamma^3 + a_4\gamma^4 + \mathcal{O}(\gamma^5). \quad (\text{C15})$$

Again, we estimate the local minima below the critical coupling, which are

$$\gamma_1 = 0 \vee \gamma_2 = -\frac{3a_3}{8a_4} + \sqrt{\left( \frac{3a_3}{8a_4} \right)^2 - \frac{a_2}{2a_4}}. \quad (\text{C16})$$

By equating  $E(\gamma_2) = 0$ , we find the relation

$$4a_2a_4 - a_3^2|_{\lambda=\lambda_{a1}} = 0 \quad (\text{C17})$$

- 
- [1] B. Vogell, K. Stannigel, P. Zoller, K. Hammerer, M. T. Rakher, M. Korppi, A. Jöckel, and P. Treutlein, *Phys. Rev. A* **87**, 023816 (2013).
  - [2] A. Jöckel, A. Faber, T. Kampschulte, M. Korppi, M. T. Rakher, and P. Treutlein, *Nature Nano.* **10**, 55 (2015).
  - [3] H. Zhong, G. Fläschner, A. Schwarz, R. Wiesendanger, P. Christoph, T. Wagner, A. Bick, C. Staarmann, B. Abeln, K. Sengstock, and C. Becker, *Rev. Sci. Instrum.* **88**, 023115 (2017).
  - [4] P. Christoph, T. Wagner, H. Zhong, R. Wiesendanger, K. Sengstock, A. Schwarz, and C. Becker, *New J. Phys.* **20**, 093020 (2018).
  - [5] A. Vochezer, T. Kampschulte, K. Hammerer, and P. Treutlein, *Phys. Rev. Lett.* **120**, 073602 (2018).
  - [6] N. Mann, M. Reza Bakhtiari, A. Pelster, and M. Thorwart, *Phys. Rev. Lett.* **120**, 063605 (2018).
  - [7] K. Hammerer, M. Aspelmeyer, E. S. Polzik, and P. Zoller, *Phys. Rev. Lett.* **102**, 020501 (2009).
  - [8] K. Hammerer, M. Wallquist, C. Genes, M. Ludwig, F. Marquardt, P. Treutlein, P. Zoller, J. Ye, and H. J. Kimble, *Phys. Rev. Lett.* **103**, 063005 (2009).
  - [9] M. Wallquist, K. Hammerer, P. Rabl, M. Lukin, and P. Zoller, *Phys. Scr.* **T137**, 014001 (2009).
  - [10] M. Paternostro, G. De Chiara, and G. M. Palma, *Phys. Rev. Lett.* **104**, 243602 (2010).
  - [11] C. Genes, H. Ritsch, M. Drewsen, and A. Dantan, *Phys. Rev. A* **84**, 051801(R) (2011).
  - [12] B. Vogell, T. Kampschulte, M. T. Rakher, A. Faber, P. Treutlein, K. Hammerer, and P. Zoller, *New J. Phys.* **17**, 043044 (2015).
  - [13] H. K. Lau, A. Eisfeld, and J. M. Rost, *Phys. Rev. A* **98**, 043827 (2018).



- [14] C. F. Ockeloen, R. Schmied, M. F. Riedel, and P. Treutlein, *Phys. Rev. Lett.* **111**, 143001 (2013).
- [15] E. S. Polzik and K. Hammerer, *Ann. Phys. (Berlin)* **527**, A15 (2015).
- [16] S. Yi and H. Pu, *Phys. Rev. Lett.* **97**, 020401 (2006).
- [17] Y. Kawaguchi, H. Saito, and M. Ueda, *Phys. Rev. Lett.* **97**, 130404 (2006).
- [18] K. Baumann, C. Guerlin, F. Brennecke, and T. Esslinger, *Nature* **464**, 1301 (2010).
- [19] J. Klinder, H. Keßler, M. Reza Bakhtiari, M. Thorwart, and A. Hemmerich, *Phys. Rev. Lett.* **115**, 230403 (2015).
- [20] D. Nagy, G. Szirmai, and P. Domokos, *Eur. Phys. J. D* **48**, 127 (2008).
- [21] C. Maschler, I. B. Mekhov, and H. Ritsch, *Eur. Phys. J. D* **46**, 545 (2008).
- [22] M. Reza Bakhtiari, A. Hemmerich, H. Ritsch, and M. Thorwart, *Phys. Rev. Lett.* **114**, 123601 (2015).
- [23] T.-L. Ho, and V. B. Shenoy, *Phys. Rev. Lett.* **77**, 3276 (1996).
- [24] J. Sabbatini, W. H. Zurek, and M. J. Davis, *Phys. Rev. Lett.* **107**, 230402 (2011).
- [25] M. I. Merhasin, B. A. Malomed, and R. Driben, *J. Phys. B* **38**, 877 (2005).